

INFLUENCE OF BARITE AGGREGATE FRIABILITY ON MIXING PROCESS AND MECHANICAL PROPERTIES OF CONCRETE

M.A. González-Ortega*, S.H.P. Cavalaro, A. Aguado

Department of Construction Engineering, Universitat Politècnica de Catalunya, UPC-BarcelonaTech, Spain

*Corresponding author

UNIVERSITAT POLITÈCNICA DE CATALUNYA

C/ Jordi Girona 1-3

Módulo C4, planta sótano, Despacho 1

08034 Barcelona – Spain

Tel.: +34-93-401-7458; fax: +34-93-401-1036

E-mail address: gonzalezortega.ma@gmail.com

ABSTRACT:

The main objective of this paper is to evaluate the friability of the barite aggregate during the mixing process and its influence on the fresh and hardened properties of concrete. Three types of aggregates were studied: barite (in two states, dry and wet), limestone and EAF slag. A specific test was designed in which each type of aggregate was exposed to several times of mixing to evaluate possible changes to the grading curves and in the surface of the aggregates grains. Moreover, four types of concretes were designed (two with barite, one with EAF slag aggregate and one with conventional limestone aggregate) to evaluate the repercussion of this phenomenon on the fresh and hardened state properties. The results show that the mixing process modifies the grading curve of the barite at a higher extent than in the case of the other aggregates. This also has repercussion in the properties of concrete, which shows increased workability as well as poorer compressive strength and elastic modulus. The observations from the study help to explain this behavior and provide important guidelines for the design, the production and the use of barite as an aggregate for concrete.

KEYWORDS: *Barite; Friability; EAF slag aggregates; Mechanical properties*

1. INTRODUCTION

Barite is a mineral known for centuries and used in numerous applications, with increasing production levels. In 2012, global production totaled 8.4 million tonnes. The country that had the highest production level was China, with 47% of total global production, followed by India with 16.7%, the USA and Morocco with 7.7% each. Over the coming years, barite production is expected to show slow but constant growth. It is estimated that production in 2015 will reach an approximate figure of 8.52 million tonnes [1].

Among other applications, barite is used as an aggregate in concrete or mortar to increase their density [2] and for radiological protection by absorption or diffraction of radiation [3, 4]. This type of concrete or mortar is used as shielding in nuclear power stations, in particle accelerators, research reactors, medical facilities [2, 5-9] and for the immobilization of radioactive waste (the isolation of radionuclides from the environment) [3].

Despite its good properties for shielding, the ACI indicates that barite presents a highly crystalline structure that makes it a friable material. Therefore, it is prone to fragmentation when subjected to abrasion or external forces [10], which may have a negative impact on the mechanical properties of mortar or concrete produced using such aggregates. Studies performed on mortar confirm that the compressive and flexural strengths of are reduced as the percentage of barite increases, although the radiation absorption coefficient increases [4]. The abrasion could even occur before the concrete has hardened, that is, due to the energy introduced during the mixing process. This could modify the grading curve and generate a fine powder around the aggregate grains, thus affecting the properties of the interfacial transition zone.

The main objective of this paper is to evaluate the barite aggregate friability during the mixing process and the effect of such aggregate on the mechanical properties of concrete. For that, an experimental program divided in two phases was performed. The first of them emphasizes on the repercussion of the mixing time on the surficial aspect and the grading curve. A simple test was used to assess the behavior of barite in comparison with other aggregates. In the second phase, an experimental program was performed with concrete mixes in order to evaluate the influence of barite on the fresh and the hardened state properties. The conclusions derived from this study represent an advance on the knowledge of barite aggregate, providing relevant information and guidelines for the future use of the material.

2. EXPERIMENTAL PROGRAM

2.1. Materials

In total, three aggregates types were characterized in the experimental program. The aim was to compare the behavior observed in the case of barite with alternative ones used in conventional concrete or in heavyweight concrete. The barite is the focus of the study, being supplied by the Mineralia Minerals Girona S.A. quarry in Spain. The EAF slag represents the alternative high density aggregate also applied for shielding of radiation and for heavyweight concrete with slightly smaller performance than Barite [11-22], obtained from a plant belonging to ArcelorMittal in Zaragoza (Spain). The limestone aggregate is considered the reference since it is widely used in normal and high-strength concrete, being extracted from a quarry in Pallejá, Barcelona. Table 1 shows the physical properties of these aggregates.

Aggregate type	Size (mm)	Density (kg/m ³)	Average density (kg/m ³)	Water absorption (%)	Average Los Angeles loss (%)
----------------	-----------	------------------------------	--------------------------------------	----------------------	------------------------------

Barite	All-in-one	0-20	4,410	4,410	0.30	40
EAf slag	Fine sand	0-20	3,500	3,500	1.49	20
Limestone (L)	Fine sand	0-2	2,680	2,640	0.89	30
	Fine sand	0-4	2,690		0.90	
	Fine gravel	4-10	2,640		0.74	
	Gravel	10-20	2,600		0.91	

Table 1: Physical properties of the aggregates used

As expected, the barite presents the highest average density that was respectively 26% and 67% bigger than the density of EAF slag and limestone aggregate. The smallest water absorption was observed for the barite, as a consequence of its crystalline and compact microstructure. The highest absorption was measured for the EAF slag, especially in the 0-6.3 fraction. Furthermore, the results from the Los Angeles [23] test confirm that barite has the highest friability, followed by the limestone and the EAF slag.

The barite and the EAF slag come in an all-in-one grading ranging from 0 to 20 mm (0-20 according with the notation adopted). On the other hand, several grading ranges of the limestone aggregate (0-2, 0-4, 4-10 and 10-20) were mixed to compose a grading curve that approaches that of barite. The intention with this procedure is to avoid introducing variables in addition to the geologic nature of the aggregate, which could hinder the comparison of the results. The grading curves measured according with standard EN 933-1:2012 [24] are shown in Fig. 1. Although small differences appear for grains with the grading sizes between 0.2 mm and 1 mm, in general similar curves are obtained.

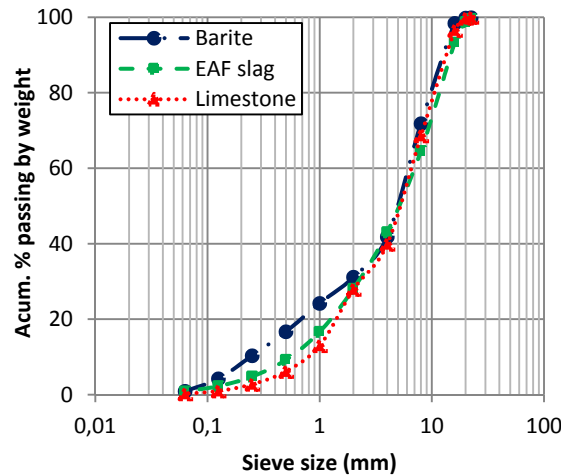


Fig. 1: Grading curves for each aggregate

Fig. 2 shows the surficial aspect and the X-Ray diffraction of all aggregates. The barite presents a surface with white-colored flakes. It is composed by 96% barium sulphate (BaSO_4), which is a mineral with a crystalline microstructure, and approximately 2% of quartz (SiO_2). On the contrary, the limestone shows a slightly rough surface. It is composed mainly by calcite (CaCO_3) and presents small amounts of quartz (SiO_2). The EAF slag has a very rough surface with cavities produced during the cooling process. It

consists of wüstite (FeO), alite (C_3S), larnite (C_2S) and gehlenite ($\text{Ca}_2\text{MgSi}_2\text{O}_7$). It also has traces of quicklime (CaO) and quartz (SiO_2). It is important to remark that the EAF slag just extracted from the furnace usually presents high contents of CaO . When mixed with water, this compound may hydrate, producing expansions [25-28]. Since this could have negative repercussion in hardened concrete, the EAF slag is subject to a stabilization process known as ageing that promotes the hydration of CaO before any use [11].

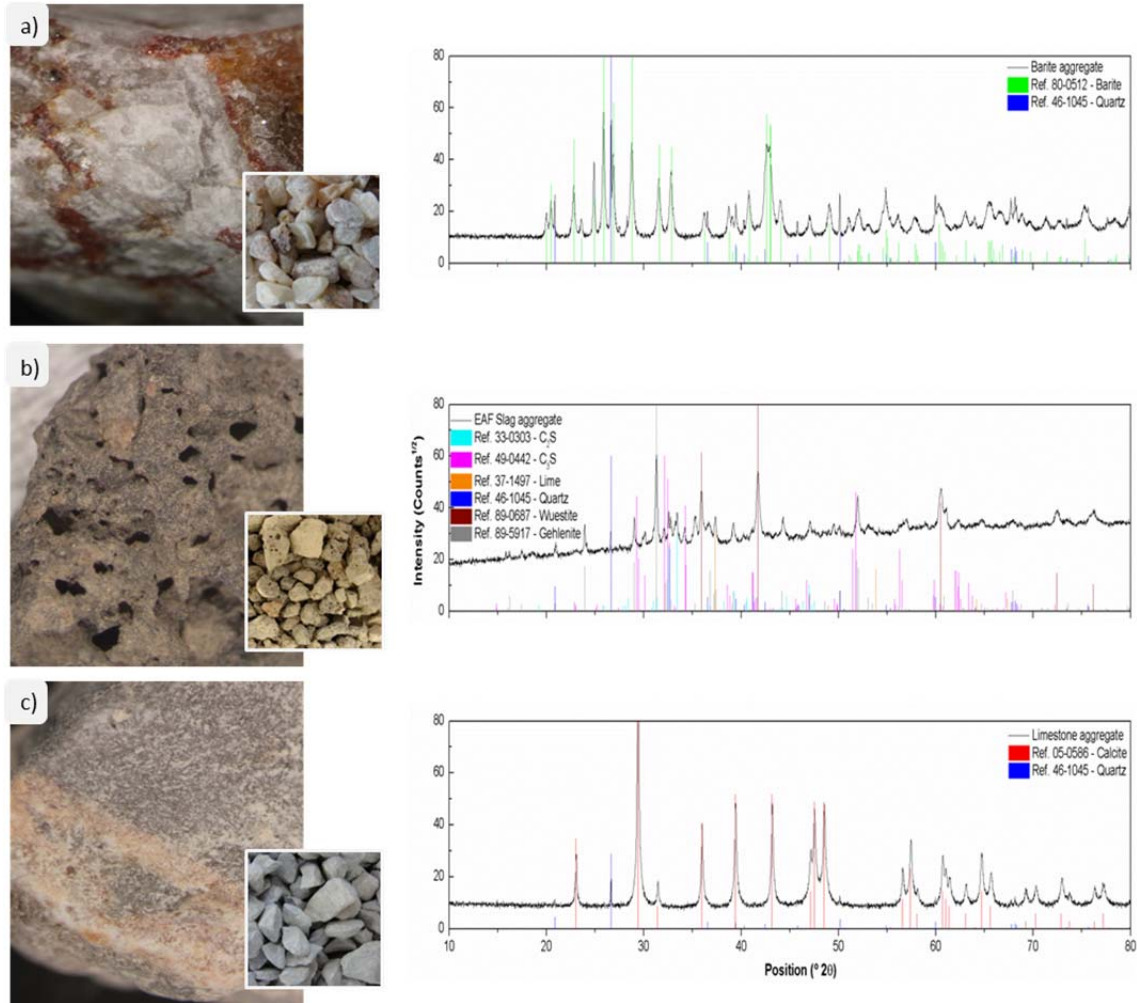


Fig. 2: surficial aspect and X-Ray diffraction of Barite (a), EAF slag (b) and Limestone aggregate (c)

2.2. Phase I: Influence of mixing process

The aim of the Phase I is to evaluate the influence of the mixing process in the surface aspect and the grading of the aggregates. Prior to initiating the tests, all aggregates were washed out to eliminate the fine particles, dried and left to rest until the equilibrium with the ambient relative humidity was reached. Then, the material was reduced into 4 approximately even samples of 40 kg according with the standard EN 932-2:1999 [29]. One of the samples of each aggregate was reduced 3 times more to obtain 5 kg subsamples. The aim here was to assess the initial grading curve in accordance with standard EN 933-1:2012 [24]. After that, the 5 kg were returned to the containers with

the remaining aggregate. Next, each sample was mixed for 30 seconds in a 1.1 kW concrete mixer with a 40-litre capacity. After this period, the grading curve was assessed again and the visual inspection was carried out. The same procedure was repeated for total mixing times of 75, 135, 255 and 435 seconds. Some grains were extracted from the samples at each time and inspected with a stereoscopic magnifying glass.

In addition to performing the test in equilibrium conditions, other samples of barite were tested in saturated conditions in order to evaluate the influence of the water on the friability of the material during mixing. In this case, the samples were wetted with 1.4 liters of water, applying a gentle manual movement of the particles to homogenize the water distribution. Immediately afterwards, it was mechanically mixed for 30 seconds and left to dry for two days. The grading curve was then obtained. This was performed for the mixing times mentioned previously.

2.3. Phase II: fresh and hardened state properties of concrete mixes

An experimental program was performed to assess the influence of the barite on the fresh and hardened state properties of concrete. For that, four types of concrete were prepared: two with barite (HABa and HABb), one with EAF slag (HS) and one with limestone aggregate (HC). Table 2 shows their composition. Notice that the difference between HABa and HABb lays only on the water content, which was modified to account for possible variations in the workability. Due to the fact that the EAF slag contain a small amount of fine granulated material, 300 kg/m³ of corrective limestone sand (0/2 mm) was added to improve workability of the mix HS. In all cases, CEM II/A-L 42.5R, a multi-use plasticizer (Melcret PF-75) and a polycarboxylate superplasticiser (Visconcrete 5940) were used.

Component		HC	HS	HABa	HABb
CEM II/A-L 42,5 R		275	275	275	275
Barite	0/20	--	--	3,204	3,204
	0/4	--	1,130	--	--
	4/10	--	136	--	--
	10/20	--	831	--	--
EAF slag	0/2	--	300	--	--
	0/4	1,003	--	--	--
	4/10	165	--	--	--
	10/20	773	--	--	--
Limestone (L)					
Water		145	140	140	123
Viscocrete 5940		0.83	0.83	0.83	0.83
Melcret PF - 75		1.93	1.93	1.93	1.93

Table 2: Mix designs of concrete types with different aggregates (Kg/m³)

The density of each concrete was recorded in compliance with standard EN 12390-7:2009 [30]. The compressive was measured according with the standard EN 12390-3:2009 [31] in two cylindrical specimens with $\phi 15 \times 30$ cm at the ages of 7, 28 and 90 days. The static and dynamic modulus were determined at 90 days, in line with standard UNE 83316:1996 and standard EN 12504-4:2006, respectively [32, 33].

3. RESULTS AND DISCUSSION

3.1. Phase I: Influence of mixing process

Table 3 summarizes the percentage by weight of material retained by each sieve at different mixing times for the EAF slag (EAF), the limestone (L), the dry (Bd) and the wet (Bw) barite.

Type	Time (s)	Size (mm)											
		filler	0.063	0.125	0.25	0.5	1	2	4	8	16	20	22.4
EAF	0	0.85	1.39	2.53	4.43	7.45	11.41	14.99	21.51	28.72	5.45	0.81	0.45
	30	1.02	1.40	2.67	4.57	7.69	11.59	14.23	21.14	27.28	7.06	1.36	0.00
	75	1.24	1.47	2.92	4.90	8.22	12.30	14.91	20.98	24.97	7.78	0.31	0.00
	135	1.05	1.50	3.13	4.94	8.38	12.62	15.61	21.57	25.21	3.37	2.61	0.00
	255	1.38	1.94	3.71	5.62	9.01	12.70	14.88	20.52	24.55	5.33	0.00	0.38
	435	1.58	1.46	3.35	5.10	8.27	11.81	14.51	21.88	25.78	6.27	0.00	0.00
L	0	0.21	0.75	1.80	3.40	6.81	14.92	12.00	28.69	27.95	3.22	0.25	0.00
	30	0.27	0.96	2.30	3.99	7.72	15.88	11.85	26.59	27.70	2.54	0.19	0.00
	75	0.23	0.77	1.80	3.13	6.34	14.14	11.83	30.25	27.96	2.33	1.22	0.00
	135	0.47	1.24	2.59	4.43	8.36	16.70	11.96	26.18	25.24	2.26	0.56	0.00
	255	0.55	0.97	2.28	3.73	7.08	15.05	11.72	27.43	28.16	3.02	0.00	0.00
	435	0.56	1.25	3.31	4.74	8.37	16.08	11.32	25.55	25.40	3.43	0.00	0.00
Bd	0	0.80	3.16	5.49	5.89	7.11	6.73	10.78	31.53	27.15	1.14	0.00	0.22
	30	1.18	3.93	7.00	6.64	7.51	6.76	9.98	27.97	27.35	1.43	0.26	0.00
	75	1.28	3.49	8.35	6.49	7.21	6.75	10.17	27.54	27.85	0.73	0.15	0.00
	135	1.20	3.50	10.35	6.72	7.18	6.97	10.36	27.59	24.61	1.21	0.32	0.00
	255	1.72	6.02	9.49	6.16	6.57	6.85	10.61	27.33	23.48	1.42	0.34	0.00
	435	1.95	7.40	9.98	5.56	5.65	6.31	10.67	27.45	23.37	1.46	0.21	0.00
Bw	0	0.99	3.53	6.71	6.80	7.96	7.11	10.63	28.42	26.00	1.71	0.13	0.00
	30	1.42	4.04	6.78	6.61	7.60	7.05	10.90	28.97	25.69	0.81	0.13	0.00
	75	1.10	2.99	8.67	5.92	6.80	6.69	10.83	29.36	26.85	0.60	0.19	0.00
	135	1.59	5.11	8.03	5.71	6.28	6.50	10.33	28.14	26.70	1.31	0.13	0.18
	255	2.46	7.36	7.92	5.16	5.60	6.48	10.83	28.04	24.80	1.33	0.00	0.00
	435	2.08	9.87	8.74	4.18	4.57	6.23	10.43	28.58	23.74	1.40	0.00	0.17

Table 3: Percentage by weight retained by each sieve at different mixing times

To simplify the analysis of the results, fig. 3 shows the curves of the percentage retained before the mixing process and after mixing for 435 seconds. A slight variation was expected due to the natural

scatter introduced by sampling and by the testing procedure. The EAF slag presents the smallest difference between its initial and final curves. This is probably the consequence of its high resistance to fragmentation (20% in the Los Angeles test) in comparison with the other aggregates. The greatest differences were observed for the wet and the dry barite, probably due to the higher friability (40% in the Los Angeles test). In both cases, a significant increase of the fraction with grading size below 0.125 mm is verified. This is compensated by a reduction in the content of coarser grading sizes.

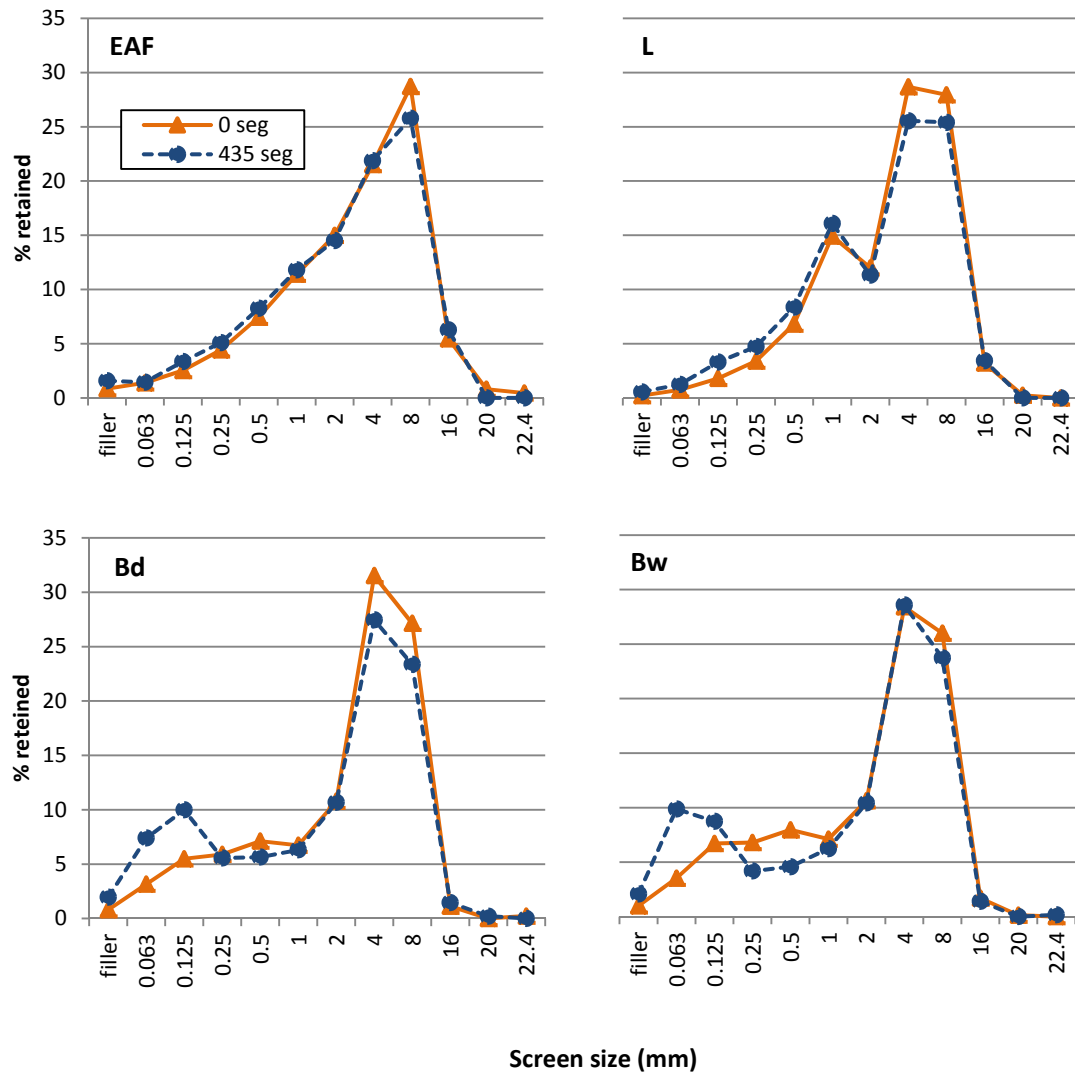


Fig. 3: Percentage retained by weight: initial and 435 seconds after mixing

Fig. 4a shows a comparison of the difference of % retained from 0 to 435 seconds depending on the grading size. Again, it is observed that the highest increases are observed for the barite with particle sizes below 0.125 mm. This is compensated by the reduction of the content of material with sizes of 0.25, 0.5, 4 and 8 mm. The results also suggest that the alteration of the grading curve of the dry barite is more pronounced than that of the wet barite.

This becomes evident in Fig. 4b that compares the relative increase of the % retained in the sieves 0.125 mm and 8 mm over time for Bd and Bw. Such relative increase is calculated for each mixing

time by dividing the difference in the % retained and the original % retained (at a time 0). Notice that variations of approximately 400% in the original retained content are observed for Bd, which is nearly half of the measured for Bw. This phenomenon may be attributed to the presence of water that contributes to the formation of a soft powder layer covering the wet barite grains. As a result, the direct interactions between particles and the alterations of the grading curve are diminished in comparison with the dry condition.

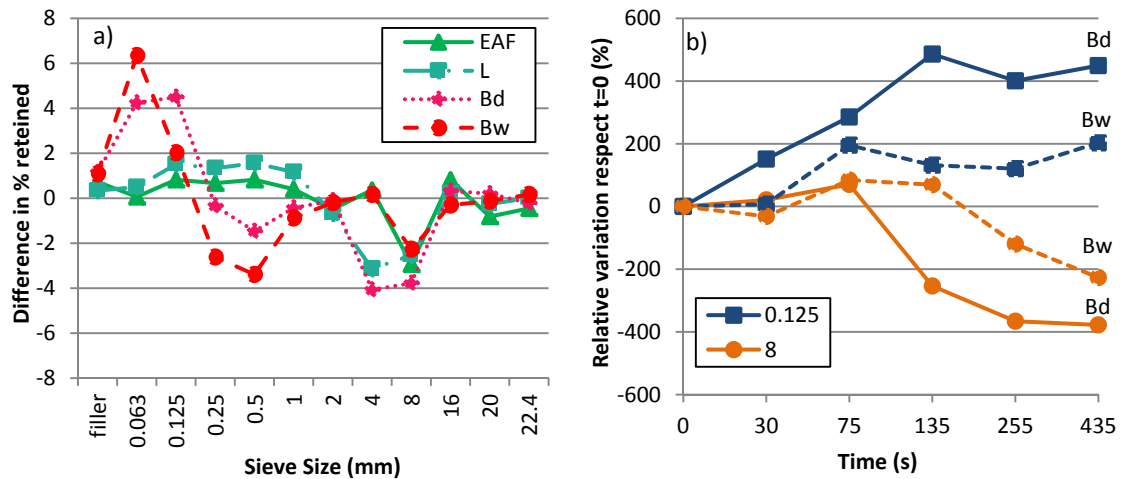


Fig. 4: Increase in % retained after 435 seconds of mixing (a) and relative increase over time (b)

Fig. 5 shows images taken with a stereoscopic magnifying glass of the barite aggregate at three times. The first of them corresponds to the initial condition in which it is possible to distinguish some veins of the aggregate. After 75 seconds of mixing (Fig. 5b) small accumulations of fines around the grain become visible. Such accumulation increases with the mixing time, reaching a condition after 435 seconds in which almost the whole surface is covered by fines. This phenomenon was observed at a much less extent in the EAF slag and the limestone aggregates given that both aggregates have practically no increase on the content of fines during the mixing process (see Fig. 3).

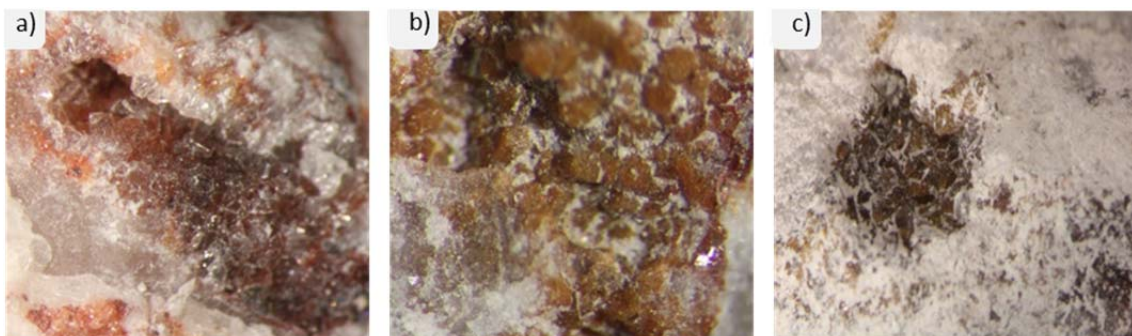


Fig. 5: Adherence of fine granules at the following times: (a) start (b) 75 seconds and (c) 435 seconds

The fact that part of the fines remains around the coarser barite grains could induce a minor systematic error on the assessment of grading curves since part of the weight of fines may be computed

as coarser grains. The proper consideration of that would lead to a slightly higher alteration of the grading curves.

The results derived from Phase I suggest that, in order to reduce the negative repercussions of barite friability during the mixing process, it is advisable to control the mixing time and the energy applied in the process. Likewise, the time spent for mixing the aggregates in dry condition should be reduced.

3.2. Phase II: fresh and hardened state properties of concrete mixes

The exfoliation of barite observed during the mixing process and the deposition of fines around the coarser grains could affect the fresh and the hardened state properties of the concrete. Table 4 summarizes the results from the tests performed with the 4 concrete mixes from Phase II.

Concrete		Slump (cm)	Occluded air (%)	Density (kg/m ³)	
				fresh	hardened
HC		3	2.9	2,406	2,388
HS		0.5	--	2,874	2,872
HAB	a	9	2.7	3,413	3,420
	b	9	2.4	3,431	3,418

Table 4: Properties of each type of concrete

The workability of the different concrete types reflects the characteristics of the various aggregates and their composition. The highest slump was obtained for the BC due to the lower water absorption and the higher content of fines, increased after the mixing process. On the contrary, the smallest slump was obtained for the HS that showed the greater absorption and the smaller fine content. The fresh and the hardened density of the concrete depend on the specific density of the aggregate. Therefore, the HAB and the HS show densities that are approximately 45% and 20% greater than that of HC.

Fig. 6a shows the average compressive strength measured. In all cases, the compressive strength increases with time. The highest values were obtained for the HS, closely followed by the HC. Interestingly, the strength measured at 7 days in both cases is bigger than the achieved by the HAB at 90 days. On average, HAB presented compressive strength 30% smaller than those of HS and HC.

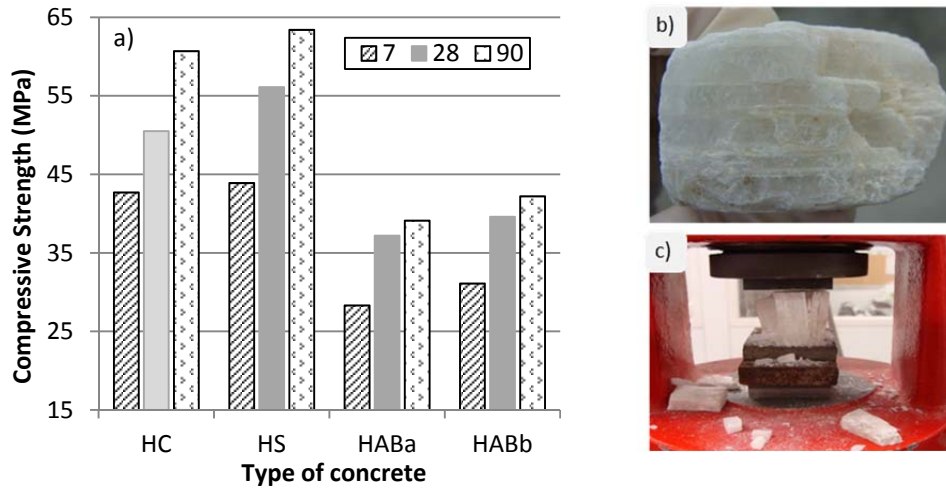


Fig. 6: Compressive strength results (a) and delamination of barite aggregate (b and c)

It is clear that the performance of HAB was conditioned by the friability and the cracking pattern experienced by the barite under compression. Its microstructure is composed of adjacent layers with interfaces, as shown in Fig. 6b. When the aggregate is subjected to a critical compression parallel to the layers, a failure due to delamination occurs at reduced load levels. Moreover, the deposition of a layer of fines around the aggregate during the mixing process observed in the results from section 3.1 could compromise the properties of the interfacial transition zone between the cement paste and the aggregate with negative repercussion in the compressive strength.

Fig. 7a shows the values of the static and dynamic modulus after 90 days for each type of concrete. This dynamic modulus calculated with the ultrasound pulse velocity is directly related with the density of the material. In practice, materials with higher density tend to present higher dynamic elastic modulus. Therefore, it was expected that the introduction of barite in the composition of concrete would lead to an increase in the dynamic elastic modulus in comparison with those with the other aggregates.

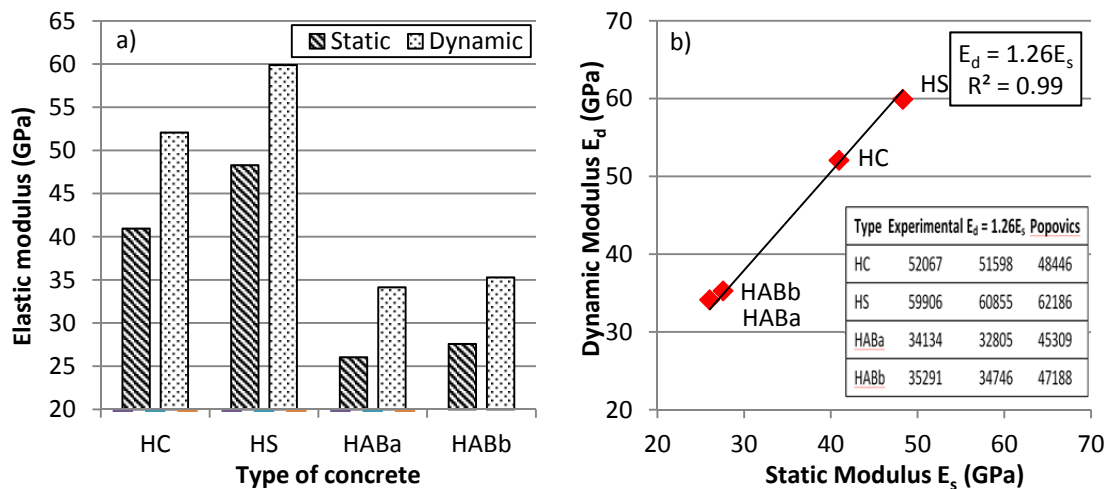


Fig. 7: Modulus of Elasticity at 90 days (a) and correlation between elastic and static modulus (b)

The results obtained contradict such assumption since HAB shows values 40% and 50% smaller than the calculated for HC and HS, respectively. This is not directly related with the nature of the barite, which is denser than the limestone aggregate and the EAF Slag. Rather than that, it is the reflex of the poor connection between the cement paste and the barite grains due to the formation of a fine dust around the aggregate during the mixing process. This creates an interface that affects that transmission of the ultrasonic pulse. The repercussion of such layer is also observed in the results of the static elastic modulus, which follow the same trend described previously. As shown in Fig. 7b, the relation between the dynamic and the static modulus follow a straight line. The former is 1.26 times the latter, with a correlation of $R^2 = 0.9936$.

The values of dynamic modulus calculated with this linear regression are compared in Fig. 7b with the estimated with the equation proposed by Popovics (1975). The latter takes into account the density and has been successfully applied for lightweight and normal concretes [34]. The results show that the equation of Popovics provides a fair prediction for HC and HS. Nevertheless, it overestimates by approximately 35% de dynamic modulus in the case of concrete with barite. This is the consequence of the atypical behavior presented by barite in comparison with other aggregates given that it presents high density associated with small elastic modulus.

4. CONCLUSIONS

The study conducted shed light on the repercussion of the friability of barite on the mixing process and on the properties of concrete. The following conclusions may be derived based on the results obtained.

- The energy introduced by the mixing process modifies the grading curve of barite. An increase in the content of material finer than 0.125 mm is observed thanks to the abrasion experienced by coarser grains. The high friability of barite is the responsible for such alterations.
- The alterations of the barite grading curve were accompanied by the formation of a fine dust layer around the grains, which becomes more evident as the mixing time increases. Since this layer might compromise the performance of the interface transition zone between paste and aggregate, it is advisable to reduce the mixing time and to control de energy applied in the process.
- The alterations of the grading curve of barite were more significant when the mixing process was performed in dry condition than in wet condition. This is probably due to the formation of a soft protective layer that reduces the interaction between wet barite grains. Therefore, the period of mixing the materials in dry condition should be reduced in order to mitigate negative repercussions.
- Concrete with barite showed greater workability than that of equivalent mixes with limestone aggregate and EAF slag. The main reason for that is the low absorption of barite and its low capacity to adsorb water.

- The introduction of barite in the concrete mixes led to a generalized reduction of the mechanical properties. Reductions from 30% to 50% in terms of the compressive strength and the elastic modulus were verified in comparison with equivalent concrete mixes with limestone aggregate and EAF slag. On one hand, this is the result of the barite microstructure, which is composed by adjacent layers that present weak planes and is prone to delamination. On the other hand, this is the consequence of the poor performance of the interface transition zone caused by the deposition of a fine dust around the aggregates during the mixing process.

ACKNOWLEDGEMENTS

The authors wish to express their gratitude to Promotora del Mediterráneo S.A, Spain (PROMSA) for supporting this work through the Research Project “Study of the behaviour of concrete manufactured with EAF steel slag” and to Mineralia Minerals Girona S.A. for supplying barite aggregates. M.A. González-Ortega acknowledges the financial support of the National Council for Science and Technology, Mexico (CONACYT). The writers thank the support of Dr. Ignacio Segura.

REFERENCES

- [1] Merchant Research & Consulting Ltd. *Barite: 2014 Market Review and Forecast*. Jan. 2014. 81 pp.
- [2] Mostofinejad D., Reisi M., Shirani A. (2012). *Mix design effective parameters on γ -ray attenuation coefficient and strength of normal and heavyweight concrete*. Constr Build Mater 2012; 28: 224-229
- [3] Shaaban I., Assi N. (2011). *Measurement of the leaching rate of radionuclide ^{134}Cs from the solidified radioactive sources in Portland cement mixed with microsilica and barite matrixes*. Journal of Nuclear Materials 2011; 415: 132-137
- [4] Binici H., Aksogan O., Sevinc A.H., Kucukonder A. (2014). *Mechanical and radioactivity shielding performances of mortars made with colemanite, barite, ground basaltic pumice and ground blast furnace slag*. Constr Build Mater 2014; 50: 177-183
- [5] Akkurt I., Basyigit C., Kilincarslan S., Mavi B., Akkurt A. (2006). *Radiation shielding of concretes containing different aggregates*. Cem Concr Compos 2006; 28: 153-157
- [6] Topçu I.B. (2003). *Properties of heavyweight concrete produced with barite*. Cem Concr Res 2003; 33: 815-822
- [7] Kilincarslan S., Akkurt I., Basyigit C. (2006). *The effect of barite rate on some physical and mechanical properties of concrete*. Materials Science & Engineering A 2006; 424: 83-86
- [8] Akkurt I., Altindag R., Basyigit C., Kilincarslan S. (2008). *The effect of barite rate on the physical and mechanical properties of concretes under F-T cycle*. Materials & Design 2008;29: 1793-1795

- [9] Sakr K., EL-Hakim E. (2005). *Effect of high temperature or fire on heavyweight concrete properties*. Cem Concr Res 2005; 35: 590-596
- [10] ACI Committee 304. *Guide for Measuring, Mixing, Transporting, and Placing Concrete*. ACI 304R-00. American Concrete Institute 2009. pp 33
- [11] González-Ortega M.A., Segura I., Cavalaro S.H.P., Toralles-Carbonari B., Aguado A., Andrello A.C. (2014). *Radiological protection and mechanical properties of concretes with EAF steel slags*. Constr Build Mater 2014; 51: 432-438
- [12] Arribas I., Vegas I., San-José J.T., Manso J.M. (2014). *Durability studies on steelmaking slag concretes*. Materials & Design. Nov 2014; 63: 168-176
- [13] Pellegrino C., Cavagnis P., Faleschini F., Brunelli K. (2012). *Properties of concretes with black/oxidizing electric arc furnace slag aggregate*. Cement & Concrete Composites 2012; 37: 232-240
- [14] Etcheberria M., Pacheco C., Meneses J.M., Berridi I. (2010). *Properties of concrete using metallurgical industrial by-products as aggregates*. Constr Build Mater 2010; 24: 1594-1600
- [15] Manso J.M., Hernández D., Milagros Losáñez M., González J.J. (2011). *Design and Elaboration on Concrete Mixtures Using Steelmaking Slags*. ACI Materials Journal 2011; 108-M72: 673-681
- [16] Arribas García, I. (2011). *Estudio y diseño de hormigones estructurales basados en la incorporación de subproductos siderúrgicos: viabilidad tecnológica*. Tesis Doctoral. Universidad del País Vasco. Bilbao.
- [17] Polanco J.A., Manso J.M., Setién J., González J.J. (2011). *Strength and durability of concrete made with electric steelmaking slag*. ACI Materials Journal 2011; 108-M22: 196-203
- [18] San-José J.T., Vegas I., Arribas I., Marcos I. (2014). *The performance of steel-making slag concretes in the hardened state*. Materials and Design. Agu 2014; 60: 612-619
- [19] Manso J.M., Polanco J.A., Losáñez M., González J.J. (2006). *Durability of concrete made with EAF slag as aggregate*. Cement & Concrete Composites 2006; 28: 528-534
- [20] Pellegrino C., Gaddo V. (2009). *Mechanical and durability characteristics of concrete containing EAG slag as aggregate*. Cement & Concrete Composites 2009; 31: 663-671
- [21] Akinmusuru J.O. (1991). *Potential beneficial uses of steel slag wastes for civil engineering purposes*. Resour Conserv Recycl 1991; 5: 73-80
- [22] Abu-Eishah S.I., El-Dieb A.S., Bedir M.S. (2012). *Performance of concrete mixtures made with electric arc furnace (EAF) steel slag aggregate produced in the Arabian Gulf region*. Constr Build Mater 2012; 34: 249-256
- [23] EN 1097-2:2010. Test for mechanical and physical properties of aggregates – Part 2: Methods for the determination of resistance to fragmentation
- [24] EN 933-1:2012. Tests for geometrical properties of aggregates – Part 1: Determination of particle size distribution – Sieving method
- [25] Vázquez-Ramonich E., Barra M. (2001). *Reactivity and expansion of electric arc furnace slag in their application in construction*. Materiales de Construcción 2001; 51: 137-148

- [26] Frías M., San-José J.T., Vegas I. (2010). *Steel slag aggregate in concrete: the effect of ageing on potentially expansive compounds*. *Materiales de Construcción* 2010; 60: 33-45
- [27] Wang G., Wang Y., Gao Z. (2010). *Use of steel slag as a granular material: Volume expansion prediction and usability criteria*. *Journal of Hazardous Materials* 2010; 184: 555-560
- [28] Frías M., Sánchez de Rojas M.I. (2004). *Chemical assessment of the electric arc furnace slag as construction material: Expansive compounds*. *Cement Concr Res* 2004; 34: 1881-1888
- [29] EN 932-2:1999. Test for general properties of aggregates – Part 2: Methods for reducing laboratory samples
- [30] EN 12390-7:2009. Testing hardened concrete – Part 7: Density of hardened concrete
- [31] EN 12390-3:2009 / AC:2011. Testing hardened concrete – Part 3: Compressive strength of test specimens
- [32] UNE 83316:1996. Concrete Tests. Determination of the modulus of elasticity in compression
- [33] EN 12504-4:2006. Testing concrete – Part 4: Determination of ultrasonic pulse velocity
- [34] Popovics, S. (1975). *Verification of relationships between mechanical properties of concrete like materials*. *Materials and Structures* 1975; 8: 183-191